2007 IEEE International Conference on
Robotics and Automation
Roma, Italy, 10-14 April 2007

Landing Motion Control of Articulated Legged Robot

Sanghak Sung and Youngil Youm

Abstract— **This paper deals with the landing motion of an articulated legged robot. Humans use a peculiar crouching motion to land safely which can be characterized by body stiffness and damping. A stiffness controller formulation is used to realize this human behavior for the robot. Using this method, the landing motion is achieved with only the desired body stiffness and damping values, without desired COG (Center of Gravity) or joint paths. To achieve soft landing, variable body stiffness and damping values were optimized.**

PBOT, which has four links with flexible joints was used for validation of the landing controller. A body stiffness and damping controller was used as an outer landing control loop and a fast subsystem controller for flexible joints was used as an inner force control loop. Simulations and experimental results about the landing motion are presented to show the performance of the body stiffness and damping controller.

Index Terms— **Legged locomotion, Landing motion, Hopping robot, Body stiffness and damping, Flexible joint**

I. INTRODUCTION

In human motion analysis, the hopping motion is usually modeled as a simple spring-mass[1], [2]. This model was been realized in robotics through various experiments by compensating energy loss using bounce of leg by Raibert[3]. After this, similar investigations were published[4], [5]. Most of them used the identical mechanical structure with some advanced features in the hopping method and in structure.

Running and hopping of the biped humanoid robot is now a very challenging area to make more agile and fast humanoid motion. There were some research efforts[6], [7] to make an articulated legged robot run by various path planning and nonlinear control techniques. In 2003, Sony realized running motion using the biped humanoid robot QRIO[8]. In 2004, Honda demonstrated running motion in the human size biped robot ASIMO[9], up to 6km/h . In [8], a method for acquiring an analytical solution of the x-,y- COG path considering angular momentum using dynamic boundary conditions is presented for the running motion. In [10], the desired angular and linear momentum is calculated from a predetermined COG and the robot is controlled through the developed controller. However, a limitation of these previous studies about humanoid motion was that controller follows the desired COG path or dynamic boundary condition provided by the operator. This can produce unexpected touchdowns so that the COG path must be corrected to ensure motion stability because of the difficulty in predicting impact time and robot state after impact. In the case of running and landing motion of humans, the characteristic named body stiffness and damping is used[13] to hop or land. It is known that a human behaves like a spring at the beginning of the impact and changes behavior into damping characteristics.

Sanghak Sung is with the Department of Mechanical Engineering, POSTECH, san31, Hyoja, Namgu, Pohang, Kyungbuk, Korea, South gotaiji@postech.ac.kr

Youngil Youm is with Faculty of Department of Mechanical Engineering, POSTECH, san31, Hyoja, Namgu, Pohang, Kyungbuk, Korea, South youm@postech.ac.kr

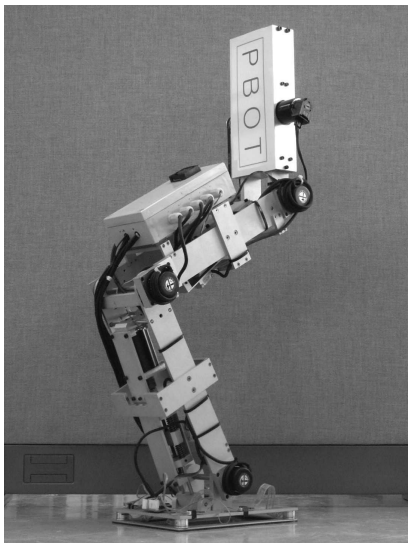

Fig. 1. Photo of PBOT

In this paper, a body stiffness and damping controller which resembles human's landing strategy will be applied to the landing motion of the legged robot, PBOT (Fig. 1) which has been made for hopping or running motion. The articulated legged robot system is treated as a lumped single mass (COG) and forces from body stiffness and damping are applied on COG as a virtual force to realize body stiffness and damping behavior. A similar approach using body compliance was tried in [11], this method also follows desired path while requiring force and acceleration sensor signals to follow the desired body impedance. On landing, instead of following a preplanned motion, adaptation to the impact phenomenon is a more important target. The method developed in this paper utilizes a simple formulation of stiffness controller which reacts to the change of external environment rather than following a preplanned path. It requires only position and velocity signals according to desired body stiffness and damping values.

The target motion is drop landing from a given height to the ground until robot stops. Constant and variable body stiffness and damping value cases will be introduced and compared. The variable value case a shows soft landing behavior which resembles a human's. In section II, we val-

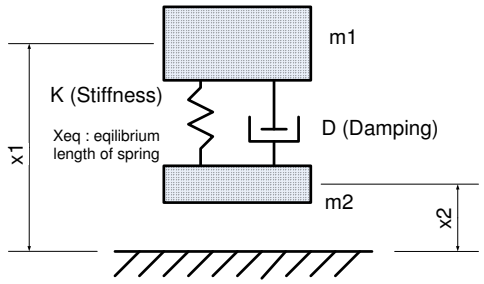

Fig. 2. 1-D two-mass system

idate the body stiffness and damping strategy using a two mass system landing simulation. Section III describes the PBOT. Section IV introduces application processes of the body stiffness and damping controller and a fast subsystem controller. Simulation results using constant and variable body stiffness and damping controller are provided. Section V shows experimental results with the PBOT.

II. Body Stiffness and Damping Behavior

A. Human's Landing Strategy

To make a landing strategy for a robot, it is important to understand the human landing strategy. It relates shock absorption of ground impact with two categories. One is shock absorption by materials using muscles, tendons and the foot heel pad. The other is shock absorption by a crouching motion, as seen at gymnastic competitions. In the latter case, impact force is transformed into another energy, like potential energy (stored at the elastic material) or kinetic energy. Also, the transferred impulse from the ground to the upper body is reduced by body crouching. In this paper, we use this motion behavior for shock absorption to make a robot land on the ground.

To apply human's behavior to the robot, we need a mathematical description of this motion. Biomechanics has explained human hopping and landing behavior using parametric study. When the human hops continually, leg stiffness value increases from touch-down to take-off with the same initial value on every instance[13]. When landing, the human behaves like a mass with a spring-damper system. Initially, a human acts like a spring but changes his action into damping.

Leg stiffness is expressed as

$$k_{leg} = \frac{F_{peak}}{\Delta L} \tag{1}$$

where F_{peak} is peak reaction force in the force platform and ΔL is vertical displacement of body's center of mass.

We can apply a similar strategy to legged robot landing control. Leg stiffness k_{leg} is changed by body stiffness k_g which is expanded from leg motion to whole body motion and force platform force F_{peak} by F_g which is the force on the center of gravity transferred from the ground.

B. Simple Model Validation

To validate the body stiffness and damping action on landing motion, a one dimensional (vertical directional) model (Fig. 2) composed of two masses is used. The upper mass (7.15kg) represents the lumped mass of the whole body (legged robot, humans, etc.) and the lower mass (0.75kg) is used to describe impact phenomenon with the ground.

To apply body stiffness, the distance between the two masses at impact is used as a equilibrium length for stiffness. Thrust force from body stiffness and damping is expressed as

$$F_{thrust} = K(x_{eq} - (x_1 - x_2)) - D(\dot{x}_1 - \dot{x}_2) \tag{2}$$

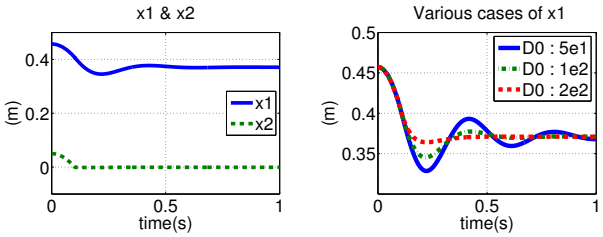

(a) Mass positions (b) Upper mass motions

Fig. 3. 1-D body stiffness and damping results

Drop landing simulation results using this thrust force with constant values of K (2000N/m, stiffness of the system) and D (200Ns/m, damping of the system) at a 0.1m initial height (x_2) is in Fig. 3(a). The two-mass system has landed on the ground using body stiffness and damping action.

The thrust force of the system enabled suppression at the ground, preventing rebound overcoming pre-transition phase which resembles the result in [14]. We also could determine motion characteristics after the initial impact with various body stiffness and damping values (Fig. 3(b)).

Reduction of impulse transfer to the upper body can be achieved through variation of these values. When these values are constant, thrust force has impulsive behavior (Fig. 4(a)). In humans, body stiffness and damping behavior changs from spring to damper, which is not constant. In [15], the joint stiffness was found to be first-order in human hopping motion. From [16], we can assume body stiffness as first-order using the result of [15]. To define variable body stiffness and damping profiles, we assume as a first-order model as follows.

$$K = K_0 + K_1 t \tag{3}$$

$$D = D_0 + D_1 t \tag{4}$$

where t is time after impact.

To determine the coefficients of body stiffness and damping for the variable case, multi-objective optimization with a simple model (Fig. 2) was used according to given constraints. An objective function for optimization can be thrust force peak minimization (because of actuator limit). Opti-

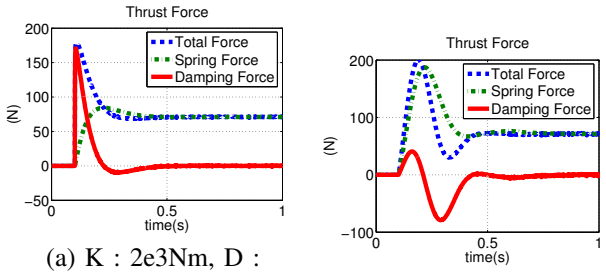

(a) K : 2e3Nm, D : 2e2Ns/m (b) Variable value case

Fig. 4. Thrust force for constant and variable K & D cases

TABLE I
OPTIMIZATION OF BODY STIFFNESS AND DAMPING VALUES

	$K0$	K_1	D_1
Case I	1500N/m	1268N/m	1388N/m
Case II	2000Ns/m	2755N/m	841Ns/m
Case III	2500Ns/m	2636/m	967Ns/m

mization constraints were selected to be:

$$\begin{aligned} \text{Minimize :} \quad & f : \text{thrust force peak} \\ \text{Subject to :} \quad & g_1 : x_1 - x_2 > x_{lower} \\ & g_2 : F < F_{max} \\ & g_3 : \dot{x}_1 > 0, \quad t_1 < t < t_2 \\ & g_4 : x_1 - x_2 < x_{st}, \quad t_1 < t < t_2 \end{aligned}$$

g_1 is used to prevent undershoot of COG below the joint limit. g_3 and g_4 are used to drive $\dot{x}_1$ to zero at steady state (x_{st}). Initial positions for drop landing are x_1 = 0.457m, x_2 = 0.05m. Time duration for stiffness and damping value change is 0.5 sec after initial impact, which is a sufficient settlement time for landing.

Initial body stiffnesses (K_0) were $1500N/m$, $2000N/m$ and $2500N/m$. Initial body damping values (D_0) were set to zero because body damping effect is not good for preventing impulse transfer to the upper body, while damping action helps absorbing high frequency shock on foot pad. In Table. I, optimized body stiffness and damping values are presented. Fig. 4(b) shows a moderate increase of thrust force. Higher order polynomial on variable body stiffness and damping was not used because of difficulty in getting solution. This section validated body stiffness and damping behavior as a landing motion controller. The next section applies this behavior to control of the landing motion of the PBOT.

III. PBOT

PBOT (Fig. 1) is a four-link (foot, shank, thigh, torso) legged robot that has 3 actuators and 8 degrees of freedom for planar motion (x, y, θ_0, θ_1, θ_2, θ_3, z_1, z_2), where z_i is a spring force coordinate for ankle and knee actuator. Linear actuation mechanism is used for the ankle and knee joints, which use series elastic actuator[12], where a ball screw and spring (60kN/m) are serially connected with a motor to allow impact shock tolerance. This linear actuator is connected to the robot by forming a closed kinematic chain around the ankle and knee joints. the hip joint is actuated by a rotary motor with gear through belt transmission. The foot is planar, with four Force Sensing Resistors (FSRs), used for touch sensing at its corners. The foot has a 2.5mm thick rubber layer on the bottom for shock absorption.

Six encoders are installed to measure joint angles and linear displacement of the springs. Absolute angle of the foot is measured through an INS (gyro) sensor. The PBOT weighs 7.9kg and stands 0.95m tall. The dimension is based on a small adult. Detailed dimensions of PBOT are in Table. II.

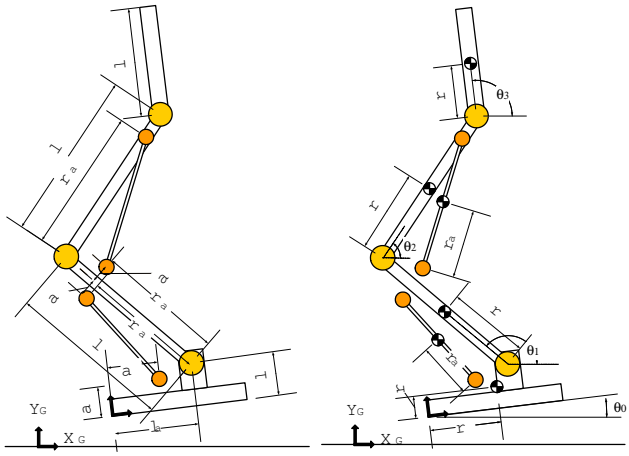

Fig. 5. PBOT model description

IV. BODY STIFFNESS AND DAMPING CONTROL FOR ARTICULATED LEGGED MODEL, PBOT

In this section, body stiffness and damping behavior is now extended to the articulated legged robot system (PBOT) for landing motion.

A. Formulation of Body Stiffness and Damping Value for PBOT

To apply body stiffness and damping behavior to the legged model, we need to define body stiffness and damping values for this system. Though there are actual springs in the PBOT, we can not change their stiffness value. Also there is no damping in actual system.

To assign desired body stiffness and damping values to the robot, a stiffness controller formulation is used. The stiffness controller is a force controller to react against external force. We use this controller to react against vertical COG motion (x_1 motion in section. II) in the landing motion. The task space is the COG point of the system. The stiffness controller is written as

$$\tau = J^T F \ (F : \text{external force}). \tag{5}$$

where J is the Jacobian about the task coordinate of the robot. To create the body stiffness and damping controller, the Jacobian is changed into a COG Jacobian[17] to decompose the desired COG force (F_g) into joint space.

TABLE II

KINEMATIC AND MASS DATA OF 4 LINK LEGGED ROBOT

Link index(link i)	0		1	2	3	actuator$_1$	actuator$_2$	
mass(kg, m_i)	0.77		1.19	1.46	2.02	1.25	1.25	
Inertia(kgm^2, I_i)	0.01		0.02	0.03	0.01	0.01	0.01	
Link Length(m, l_i)	l_0 : 0.07	l_{01} : 0.13	0.34	0.34	0.30	r_{1a1} : 0.29	r_{1a2} : 0.29	r_{2a2} : 0.30
COG Length(m, r_i)	r_{01} : 0.13	r_{02} : 0.03	0.17	0.17	0.14	r_{a1} : variable	r_{a2} : variable	

$$\begin{aligned}\tau &= J_g^T F_g = J_g^T (F_K + F_D) \\ &= J_g^T (K_g(X_{ge} - X_g) - D_g \dot{X}_g)\end{aligned} \tag{6}$$

X_g, $(x_g, y_g)^T$ is a COG position vector calculated from the foot to the COG point. X_{ge}, $(x_{ge}, y_{ge})^T$ is the equilibrium position of the COG selected according to the desired motion after landing. Using this formulation, stiffness and damping forces used in section II are replaced by virtual body stiffness and damping forces transmitted to the COG. So, the articulated legged system can be treated as a lumped mass with virtual spring and damper force.

1) Determining the COG Jacobian: The flat foot has various contact modes (toe, heel and full contact). To determine J_g, these contact conditions must be considered and underactuated joints which exist at the contact point must be treated. However, this paper calculates J_g relative to the toe reference frame to reduce computational complexity. Desired COG force in global frame is projected into the local frame (Eq. (7)) to thrust robot in the right direction. The spring force coordinate (z_1, z_2) is ignored in calculating the COG Jacobian.

$$\tau = J_g^T R(\theta_0) F_g \tag{7}$$

where $R(\theta_0)$ is a 2×2 rotation matrix around θ_0.

There are 3 actuator degrees of freedom (ankle, knee and hip) whereas the motion degrees of freedom are 2 (x_g, y_g) for body stiffness and damping controller. To avoid redundant motion, torso pitch angle (θ_3) is added as a target control variable to make the COG Jacobian 3×3 matrix.

2) Actuator Force Tracking Controller: Desired joint torques obtained from above are transformed into desired actuator forces using the closed chain kinematics [18] of the model. To follow the desired actuator forces in the flexible joint system, a force tracking controller was developed.

The ankle and knee joint of the PBOT are flexible joints which have transmission through springs. To develop a force tracking controller about those joints, we change dynamics in singularly perturbed form[19] as

$$\begin{bmatrix} M_{11} & M_{12} \\ M_{21} & M_{22} \end{bmatrix} \begin{bmatrix} \ddot{\boldsymbol{x}}_s \\ \mu \ddot{\boldsymbol{z}} \end{bmatrix} + \begin{bmatrix} C_1 \\ C_2 + \boldsymbol{z} \end{bmatrix} = \begin{bmatrix} AU \\ -BU \end{bmatrix} + \begin{bmatrix} \sum_{i=1}^{2} J_i^T F_i \\ 0 \end{bmatrix} \tag{8}$$

, where $\boldsymbol{x}_s$ is the slow variable $[x \ y \ \theta_0 \ \theta_1 \ \theta_2 \ \theta_3]^T$. And $\boldsymbol{z}$ is the fast variable $[z_1 \ z_2]^T$, where force in the springs (ankle and knee actuators). $\mu = k_s^{-1}$, where k_s is a stiffness

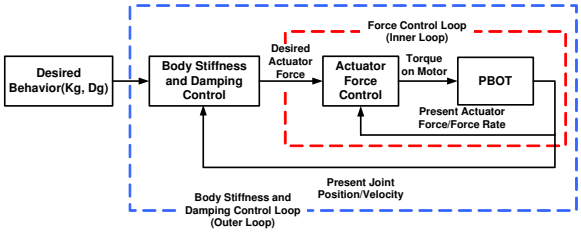

Fig. 6. Control block diagram

matrix for the spring. The C_1, C_2 matrix comprises coriolis, centrifugal and gravity forces. A is an input coefficient matrix generated from the closed chain kinematic characteristic of the system and B is a pre-multiplication matrix for input torque which is composed of gear and ball screw ratios. J_i and F_i mean the Jacobian for contact point and impact force at the contact points (toe and heel). This dynamics equation can be divided into slow and fast subsystem. Slow subsystem (upper part of Eq. (8)) represents motion of the slow variables like rigid link motion and fast subsystems (lower part of Eq. (8)) represents motion of the springs. Solving Eq. (8) for $\ddot{\boldsymbol{z}}$ gives:

$$\begin{aligned}&(M_{22} - M_{21}M_{11}^{-1}M_{12})\mu\ddot{\boldsymbol{z}} + (C_2 - M_{21}M_{11}^{-1}C1) + \boldsymbol{z} \\ &= -(B + M_{21}M_{11}^{-1}A)U - M_{21}M_{11}^{-1}\sum_{i=1}^{2} J_i^T F_i\end{aligned} \tag{9}$$

$$M_f \mu \ddot{\boldsymbol{z}} + C_f + \boldsymbol{z} = -A_f U - F_v, \text{ and} \tag{10}$$

$$\mu\ddot{\boldsymbol{z}} + M_f^{-1}C_f + M_f^{-1}\boldsymbol{z} = -M_f^{-1}A_f U - M_f^{-1}F_v, \tag{11}$$

where M_f is $(M_{22} - M_{21}M_{11}^{-1}M_{12})$, C_f is $(C_2 - M_{21}M_{11}^{-1}C1)$, A_f is $(B + M_{21}M_{11}^{-1}A)$ and F_v is the virtual external force on the fast subsystem with $M_{21}M_{11}^{-1}\sum_{i=1}^{2} J_i^T F_i$

If we select the control input U as

$$U = -A_f^{-1}(k_p(\boldsymbol{z}_d - \boldsymbol{z}) - \sqrt{\mu}k_v\dot{\boldsymbol{z}}), \tag{12}$$

where A_f^{-1} is a pre-compensator matrix for control input, Eq. (11) changes into

$$\mu\ddot{\boldsymbol{z}} + \sqrt{\mu}M_f^{-1}k_v\dot{\boldsymbol{z}} + M_f^{-1}(I + k_p)\boldsymbol{z} = M_f^{-1}(k_p\boldsymbol{z}_d - C_f - F_v). \tag{13}$$

To make the closed loop fast subsystem (Eq. (13)) asymptotically stable, all of the coefficient matrix at the left-hand side must be positive definite[20]. Since M_f^{-1} is positive definite because the determinant of a positive definite matrix (inertia

TABLE III

BODY STIFFNESS AND DAMPING VALUES ON 5, 10CM DROP LANDING SIMULATION

	x_g	y_g	θ_3
Stiffness	200N/m	2∼3000N/m	1.0N/m
Damping	100Ns/m	2∼300Ns/m	0.5Ns/m

matrix) is positive definite. If we select k_p and k_v so that the stability condition is satisfied, the fast subsystem becomes asymptotically stable while following the slow manifold. (C_f at the right hand side is composed of only slow variables and F_v is also composed of slow variables and can be characterized by impulse and step input signal to the fast subsystem dynamics.)

The force tracking controller acts as an inner force control loop for the flexible joint structure and the body stiffness and damping controller as an outer control loop (Fig. 6).

B. Drop Landing Simulation of PBOT

Our body stiffness and damping controller was implemented for drop landing simulation from a given height. Simulation conditions were based on the parameters at Table. II.

1) Constant Body Stiffness and Damping Case: To validate body stiffness and damping controller, the constant value case was tried first. x_{ge}, y_{ge} were the COG position at impact. The robot was dropped from different heights. Fig. 7 shows y_g motion path for two different dropping heights (5cm, 10cm height) using the body stiffness and damping values in Table. III. Values for torso pitch are small because of the high gear ratio at the hip actuator.

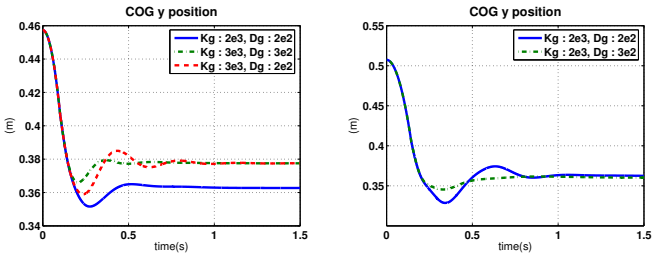

(a) 5cm foot height (b) 10cm foot height

Fig. 7. y_g for drop landing simulation

In Fig. 7(a), the y_g paths follow body stiffness and damping behavior according to the assigned values. The value of y_g around impact time (0.15s) is relatively smooth, without discontinuity, which means a soft landing. The force tracking result of ankle and knee actuator in Fig. 8 (K_g : 3000Nm, D_g : 200Ns/m) show the controller is following the desired force value except right after the impact. The tracking error is due to abrupt spring deflexion from the initial impact force. Force tracking error at the knee actuator is because of the actuator limit (0.2Nm) and the coupling effect between ankle and knee joint. Fig. 9 shows the landing simulation sequence.

Though we were not aware of the exact impact time, the robot was able to land with soft upper body motion by the assigned body stiffness and damping values. When the initial height was 10cm, y_g still behaved smoothly, but the path was rougher than the 5cm case due to the larger impact force and actuator limits (Fig. 7(b)).

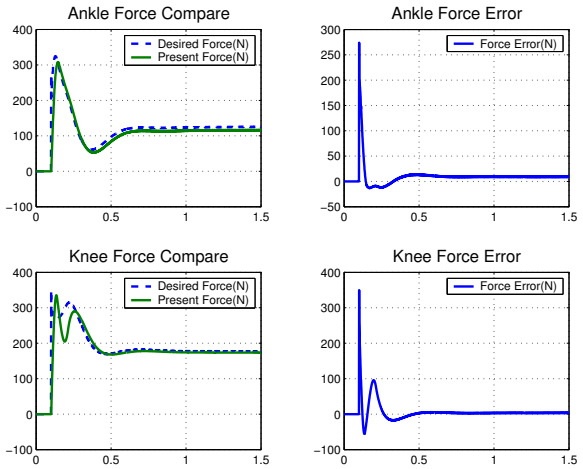

Fig. 8. Desired & present actuator force and error for 5cm drop case

2) Variable Body Stiffness and Damping Case: In variable body stiffness and damping case, the optimization result at section. II is used. The optimization result for initial body stiffness value of 2000N/m is applied to the PBOT model. Fig. 10 shows that desired actuator forces have been changed into moderate increase which is realistic result comparing with constant values cases. Ankle force tracking error was greatly reduced, but, even through the present force at the knee is slightly greater than the desired force, knee force tracking error is still relatively large due to the abrupt spring deflexion at impact.

Although the optimized values of section II do not guarantee the best simulation result because of force tracking error, we can use optimized results as an initial estimate for better landing motion.

V. EXPERIMENT WITH PBOT

Experiments have been performed using a PBOT with real time control (1KHz control frequency) using a Pentium 650MHz computer. The PBOT was dropped from arbitrary height to the ground (between 5∼10cm from the ground) by hand. All data was collected right from the initial impact.

A. Constant Body Stiffness and Damping Case

Four constant body stiffness and damping values were tested. Fig. 11 shows the experimental results of y_g. In Fig. 11(a & b), K_g is 2000N/m and 3000N/m, respectively. Both shows plots for D_g = 200Ns/m and 300Ns/m.

We can identify the body stiffness and damping behavior on landing motion according to given body behavior. The difference of steady state y_g values between the simulation (Fig. 7) and experiment (Fig. 11) is because of different equilibrium lengths for body stiffness. The initial configurations were not regular in experiments. Force tracking result when K_g is 2000N/m and D_g is 300Ns/m is in Fig. 12, which

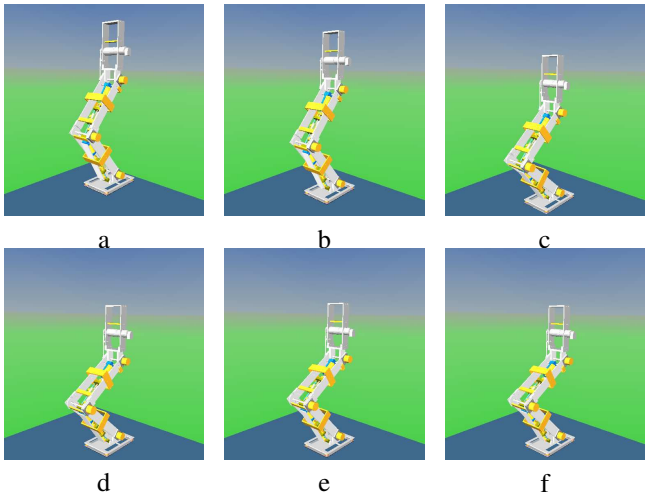

Fig. 9. Snapshots of the landing simulation

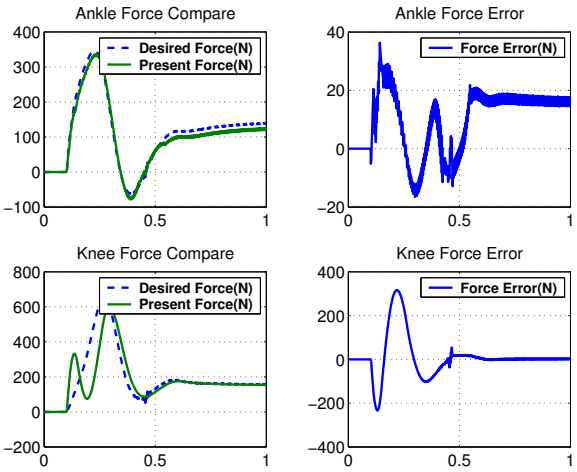

Fig. 10. Force tracking result for variable body stiffness and damping

shows more force fluctuation due to less material shock absorption than in the simulation (only 2.5mm rubber beneath the foot). Fig. 15 shows images of the landing experiment.

B. Variable Body Stiffness and Damping Case

To see the effect of variable body stiffness and damping, we used the result of Table. I, which was calculated through the optimization process of section II.

Fig. 13 shows the experimental and simulation results of y_g for various variable body stiffness and damping values. Experimental results are similar to the theoretical behaviors in simulations (two mass system case). Force tracking desired at Fig. 14 has moderate increase comparing to constant case even if there are some impulse peaks. The variable case caused a deep (long) undershoot in COG behavior compared to the constant case, which means less impulse transfer to the upper body.

VI. Conclusion

This paper has presented a body stiffness and damping controller for an articulated legged robot as a landing

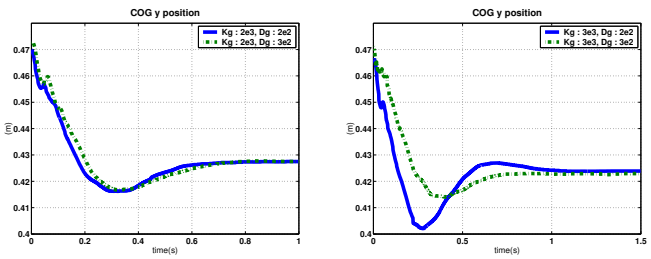

(a) y_g values-I (b) y_g values-II

Fig. 11. Drop landing experiment for four cases

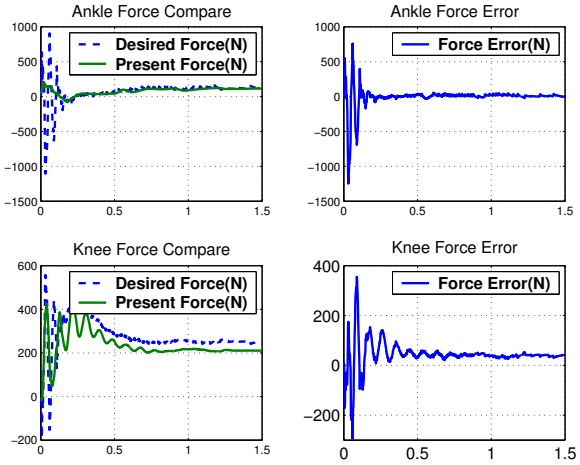

Fig. 12. Actuator force comparison, K_g : 2000N/m, D_g : 300Ns/m

controller which replicates human landing behavior. This controller has performed landing motion of the articulated legged robot system, PBOT without pre-calculated desired signals or COG paths, or prior knowledge about impact time. The controller needs only desired body stiffness and damping values and position and velocity feedback signals to control the landing motion.

Human body stiffness and damping behavior was realized through a stiffness controller formulation about the COG point. Due to the flexible joint system characteristics of PBOT, fast subsystem controller has been also developed and force tracking performance using this controller has been shown. Also, we have presented a variable body stiffness and damping case to produce a soft landing motion for upper body protection which resembles human landing behavior.

References

[1] R. Blickhan, "The spring-mass model for running and hopping, " *J. of Biomechanics*, Vol. 22, No. 11/12, pp. 1217–1227, 1989.

[2] C. T Farley and O. Gonzalez, "Leg stiffness and stride frequency in human running, " *J. of Biomechanics*, Vol. 29, No. 2, pp. 181–186, 1996.

[3] M. H. Raibert, *Legged Robots That Balance*, MIT Press, Cambridge, Massachusetts, 1985.

[4] P. Gregorio, M. Ahmadi, and M. Buehler, "Experiments with and electrically actuated planar hopping robot, ", *Experimental Robotics III*, Springer, pp. 269–281, 1994.

[5] M. D. Berkermeier, and K. V. Desai, "Control of hopping height in legged robots using a neural-mechanical approach, " *Int. Conf. on Robotics and Automation*, pp. 1695–1701, 1999.

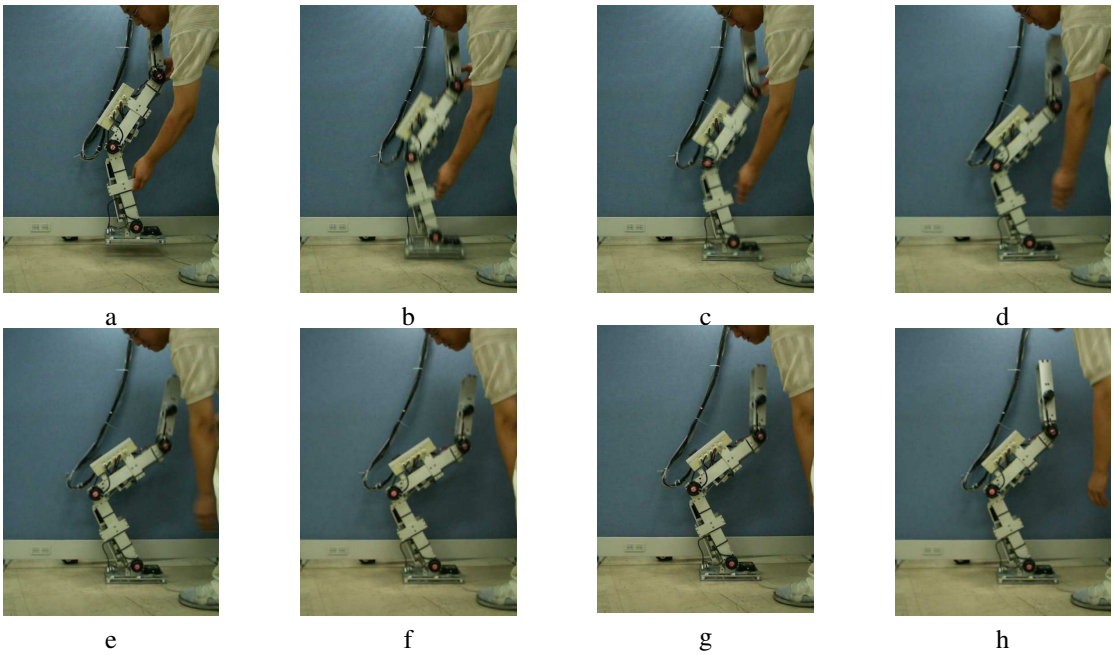

Fig. 15. Snapshots of the landing experiment

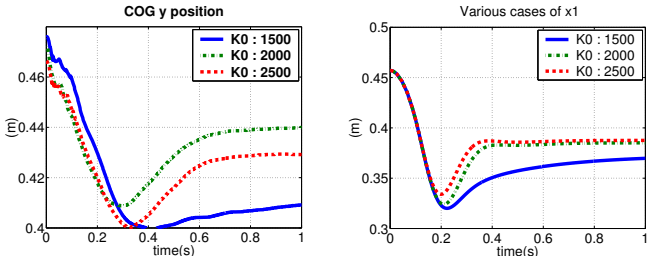

(a) Experiment result (b) Simulation result

Fig. 13. Experiment & simulation with variable body stiffness and damping

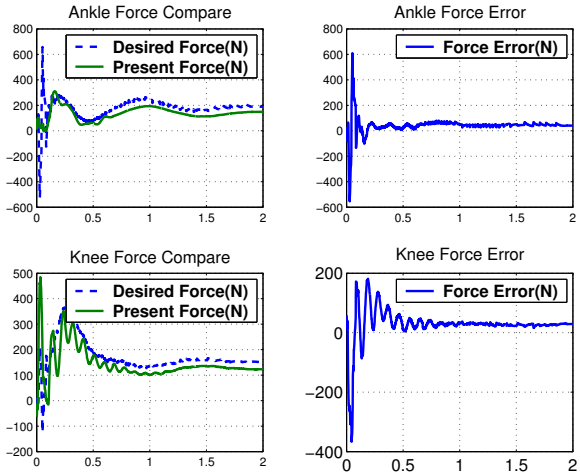

Fig. 14. Actuator force comparison of Case II in Table. I

[6] C. Chevallereau, E.R. Westervelt, and J.W. Grizzle, " Asymptotically stable running for a five-link, four-actuator, planar bipedal robot, " *Int. J. of Robotics Research*, Vol. 24, Issue. 6, pp. 431–464, 2005.

[7] J. H. Park, and O. Kwon, "Impedance control for running of biped robots, " *Int. Conf. on Advanced Intelligent Mechatronics*, pp. 944–949, 2003.

[8] K. Nagasaka, Y. Kuroki, S. Suzuki, Y. Itoh, and J. Yamaguchi, "Integrated motion control for walking, jumping and running on a small bipedal entertainment robot, " *Int. Conf. on Robotics and Automation*, pp. 3189–3194, 2004.

[9] http://www.honda.co.jp/asimo

[10] S. kajita, T. Nagasaki, K, Kaneko, K, Yokoi and K. Tanie, "A Hop towards Running Humanoid Biped," *Int. Conf. on Robotics and Automation*, pp. 629–635, 2004.

[11] E. Ohashi and K. Ohnishi, "Variable Compliance Control Based on Soft-Landing Trajectory for Hopping Robot," *IEEE Industrial Electtonics Society*, pp. 117–122, 2004.

[12] Pratt, G. A., and Willianson, M.M,"Series elastic actuators,"*Int. Conf. on Intelligent Robots and Systems*,pp. 399–406, 1995.

[13] E. B. Poul. Dyhre-Poulsen and M. Voigt, "Dynamic control of muscle stiffness and h-reflex modulation during hopping and jumping in man," *J. of Physiology*, vol. 437, pp. 287–304, 1991.

[14] N. Doh, W.K.Chung and Y.Youm, "On Hard Contact Force Control", *Int. Conf. on Intelligent Robots and System*, pp. 1528–1533, 2000.

[15] S. Rapoport, J. Mizarahi, E. Kimmel, O. Verbitsky and E. Isakov, "Constant and Variable Stiffness and Damping of the Leg Joints in Human Hopping," *J. of Biomechanical Engineering*, vol. 125, pp. 507–514, 2003.

[16] C. T. Farley and D. C. Morgenroth, "Leg stiffness primarily depends on ankle stiffness during human hopping," *J. of Biomechanical Engineering*, vol. 32, pp. 267–273, 1999.

[17] T. Sugihara, Y. Nakamura, "Whole-body cooperative balancing of humanoid robot using COG Jacobian ," *Int. Conf. on Intelligent Robots and System*, pp. 2575–2580, 2002.

[18] F. H. Ghorbel, O. Chetelat, R. Gunawardana, and R. Longchamp, "Modeling and Set Point Control of Closed-Chain Mechanisms:Theory and Eepriment," *IEEE Transaction of Control Systems Technology*, vol. 8,no. 5, pp. 801–815, 2000.

[19] Mark C. Readman, *Flexible Joint Robots*, CRC Press, 1994.

[20] LEANG S . SHIEH, MOHAMAD M. MEHIO, AND HANI M. DIB, "Stability of the Second-Order Matrix Polynomial," *IEEE Transaction on Automatix Control*, vol. AC-32, No. 3, 1987.